Chemical Science

Accepted Manuscript

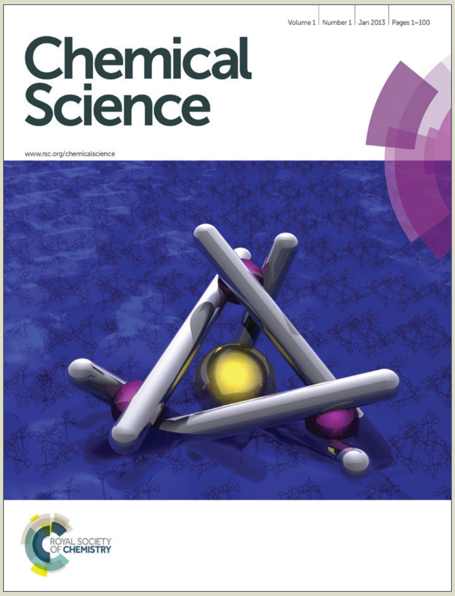

ROYAL SOCIETY OF CHEMISTRY

www.rsc.org/chemicalscience

Chemical Science RSCPublishing

ARTICLE

Aluminium-Ligand Cooperation Promotes Selective Dehydrogenation of Formic Acid to H_2 and CO_2

Cite this: DOI: 10.1039/x0xx00000x

T. W. Myers,[a] and L. A. Berben[a]*

Received 00th January 2012,
Accepted 00th January 2012

DOI: 10.1039/x0xx00000x

www.rsc.org/

ABSTRACT: Herein, we report that molecular aluminium complexes of the bis(imino)pyridine ligand, $(^{Ph}I_2P^{2-})Al(THF)X$, X = H (**1**), CH_3 (**2**), promote selective dehydrogenation of formic acid to H_2 and CO_2 with an initial turnover frequency of 5200 turnovers/h. Low-temperature reactions show that reaction of **1** with HCOOH affords a complex that is protonated three times: twice on the $^{Ph}I_2P^{2-}$ ligand and once to liberate H_2 or CH_4 from the Al-hydride or Al-methyl, respectively. We demonstrate that in the absence of protons, insertion of CO_2 into the Al-hydride bond of **1** is facile and produces an Al-formate. Upon addition of protons, liberation of CO_2 from the Al-formate complex affords an Al-hydride. Deuterium labelling studies and the solvent dependence of the reaction indicate that outer sphere β-hydride abstraction supported by metal-ligand cooperative hydrogen bonding is a likely mechanism for the C-H bond cleavage.

Introduction

Aluminium-catalyzed reactions include notable large scale processes in the chemical industry.[1] For much of this chemistry it is the ability of aluminium to facilitate both insertion and β-hydride transfer that makes catalysis possible.[2] For example, the Meerwein-Pondorf-Verley (MPV) reduction of ketones by alcohols relies on a β-hydride transfer to an acceptor alcohol substrate, and the polymerization of ethylene proceeds via repeated insertion of monomer into a growing polymer chain. Furthermore, recent work indicates that under normal reaction conditions for propagation, chain termination likely occurs via β-hydride transfer to monomer, although historically the accepted mechanism for chain termination was β-hydride abstraction and this can occur under certain reaction conditions.[3,4] Given the abundance of Al in the earth's crust and its low cost,[5] there is significant incentive to extend the catalytic chemistry of aluminium to a broader scope of transformations, and to achieve this goal a broader array of elementary reaction steps would be needed.[6]

β-Hydride abstraction, which results in formation of an Al(III)-hydride, has also been proposed in several reports of the aluminium-mediated dehydrogenation of amine-boranes, and could facilitate the dehydrogenation of other subtstrates. In the amine-borane examples, both bulky Al(III) complexes,[7] and Al(III)-based frustrated Lewis pairs,[8] affect the dehydrogenation of amine-boranes: the most effective of these catalysts perform up to 200 turnovers over a 44 h period.[8] The dehydrogenation of amine-borane involves breaking the relatively weak B-H bond rather than the stronger C-H bond present in organic substrates but the mechanistic similarities of the reaction are otherwise apparent. β-Hydride abstraction has also been reported in stoichiometric reactions of Al(III) where the steric bulk of various alkyl ligands is thought to promote the formation of aluminium-hydride products.[9]

We have found that the dehydrogenation of formic acid can be used to demonstrate that molecular complexes of the Al(III) ion can support an outer sphere β-hydride abstraction pathway, promoted by interactions of the substrate with both metal and ligand, and that results in formation of an Al(III)-hydride. Formic acid is a non-toxic liquid that affords H_2 and CO_2 if it can be dehydrogenated selectively, and it is thus a potential hydrogen storage material.[10] The importance of selective formic acid dehydrogenation is also illustrated by the significant efforts devoted to catalysis of the reaction in recent years. Some of the best catalysts for conversion of formic acid to H_2 and CO_2 are molecular Ir complexes.[11] However, efforts to develop selective catalysts based on cheaper and more abundant metals have received significant attention. Investigations in this area have resulted in catalysts based on ruthenium,[12] and more recently, rhodium and rhenium.[13,14] Advances in 1st row transition metal chemistry have afforded cobalt- and iron-based catalysts.[15,16]

Herein we present selective formic acid (HCOOH) dehydrogenation by a molecular aluminium complex that proceeds with an initial rate of 5200 turnovers/h. We describe experiments that characterize each of the elementary steps in the catalytic cycle. We establish that the aluminium-ligand cooperative activation is responsible for the initial deprotonation of formic acid, and then using deuterium labelling studies, we show that an outer sphere β-hydride abstraction from formate results in formation of an Al-hydride, and liberation of CO_2 under acidic reaction conditions. We also provide experimental evidence to support a model where hydrogen bonding between the protonated iminopyridine ligand and the formate substrate provide stabilization of the transition state for β-hydride abstraction (wherein the C-H bond in HCOOH is cleaved). These results point to catalyst design features that could enable development of future generation aluminium-based catalysts for transformations involving acceptorless outer sphere β-hydride abstraction.

Results and Discussion

Synthesis of catalysts. We have found that aluminium hydride and aluminium-methyl complexes based on the phenyl-substituted bis(imino)pyridine ligand (henceforth denoted ${}^{Ph}I_2P$) are effective molecular aluminium catalysts for the dehydrogenation of formic acid (Figure 1). Synthesis of each of the complexes, $({}^{Ph}I_2P^{2-})Al(THF)H$ (**1**), and $({}^{Ph}I_2P^{2-})Al(THF)Me$ (**2**), was approached via a salt metathesis route in which the two-electron reduced sodium salt of the ligand, $Na_2{}^{Ph}I_2P$, was generated in situ and subsequently reacted with an appropriate aluminium salt, either $AlCl_2H$ or $AlCl_2Me$, respectively. The synthesis of **1** following this general procedure has been previously reported by us,[17] and the synthesis of **2** has now also been successfully accomplished (Figure 1, S1). Two-electron reduced ${}^{Ph}I_2P$ is diamagnetic and the ^1H-NMR spectrum of **2** definitively identified its structure. Combustion analysis confirmed the expected formulation for the molecule.

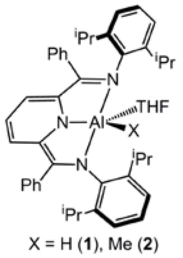

Figure 1. $({}^{Ph}I_2P^{2-})Al(THF)X$, where X = H (**1**) and CH_3 (**2**).

Catalytic dehydrogenation of Formic Acid (HCOOH). Initial experiments indicated to us that **1** and **2** are both effective molecular aluminium catalysts for conversion of HCOOH selectively into H_2 and CO_2. In refluxing THF solution, dehydrogenation of the amine adduct of formic acid, $HCOOH{:}Et_3N$ (5:2), was found to proceed rapidly in the presence of 0.006 mol. % of either **1** or **2**, with an initial rate of 5200 turnovers/h (Table 1). The TON's for the reactions catalysed by **1** and **2** reached 2200 and 2000 respectively, over 1 h of reaction, as observed using a GC with thermal conductivity detector (TCD). Notably, no CO gas was detected during any catalytic run. Control experiments including no added catalyst indicated that, under the conditions of our experiment in refluxing THF, $HCOOH{:}Et_3N$ (5:2) underwent no appreciable conversion to H_2 and CO_2 (Figure S2).

Table 1. Selective Al-catalysed conversion of HCOOH into H_2 and CO_2 performed under conditions where reaction rate is independent of HCOOH concentration (generally > 7.6 M HCOOH). Catalyst loading is 0.006 mol. %. Initial TOF, reported in turnovers/h, was measured over the first 15 minutes.

	Additive	Solvent	T/°C	TOF[a]	TON$_{1h}$[b]
1	NEt_3	THF	65	5200	2200
2	NEt_3	THF	65	4800	2000
1	NEt_3	DME	85	1100	700
1	NEt_3	diglyme	100	2400	1050
1	NEt_3	toluene	100	80	65
1	None	THF	65	220	70
1	None	toluene	100	26	8

[a] TOF is reported to be consistent with other recent reports of HCOOH dehydrogenation. More detailed information on rate constants is given in the supporting information (Table S1).[18,19] [b] TONs are reported after 1 h. All data are the average of at least two catalytic runs.

Experiments were performed to identify the best reaction conditions for using **1** as a catalyst during 1 h reactions. We investigated different solvent systems using the amine adduct of formic acid, $HCOOH{:}Et_3N$ (5:2), and found lowered initial TOFs and TONs in both DME and diglyme and further lowered TOFs and TONS in non-polar toluene, as compared with THF (*vide supra*) (Table 1). Dehydrogenation of HCOOH using **1** as the catalyst was also probed using anhydrous formic acid in place of $HCOOH{:}Et_3N$ (5:2). In THF just 70 turnovers were observed under these conditions.

Additional information about the mechanism for dehydrogenation of HCOOH by **1** was gathered from kinetic experiments which revealed the rate of reaction to be first order in catalyst and pseudo first order in formic acid (Figures S3, S4). The rate of reaction saturated at concentrations above ~7.6 M in formic acid. Variable temperature experiments allowed for the estimation of activation parameters for comparison to other catalytic systems. The reaction had a$\Delta H^{\ddagger}$ of 60.6 kJ/mol and $\Delta S^{\ddagger}$ of -84.8 J/mol which is consistent with other reported reactions with an ordered transition state (Figure S5).[16] We have also performed experiments that allowed us to characterize the reaction intermediates that form upon initial formic acid activation by **1**, and deuterium labelling experiments that illustrate that β-hydride abstraction of the formate C-H bond by Al is responsible for CO_2 liberation during catalysis (*vide infra*).

Characterization of Initial Reaction Intermediates. We performed experiments designed to identify the initial species formed in the catalytic cycle for dehydrogenation of HCOOH by **1** and **2** by performing reactions at low temperature to slow the reaction kinetics. During the experiments, the contents of the reaction were monitored by GC-TCD to detect headspace gases and, in a separate experiment, by ^1H-NMR to detect the molecular aluminium intermediates. Using 0.025 mol % of **1** for dehydrogenation of $HCOOH{:}Et_3N$ (5:2) in THF, a reaction was performed at -25° C in a sealed vessel to detect the first gaseous product of the reaction: one equivalent of H_2 was detected using GC-TCD before any CO_2 was observed (Figure S6). To probe the generality of this result, the experiment was repeated using **2** as catalyst: in that case, one equivalent of methane gas was detected initially. These results point to a common reaction intermediate for catalysis by either 1 or **2**, and explain the observed, similar initial rates of catalysis.

Further experiments were performed to understand the reactions that lead to protonoloysis of **1** and **2**. A stoichiometric reaction between **1** and 1 equivalent of HCOOH:NEt$_3$ (5:2) was performed at -25 °C in THF solution. The ^{1}H-NMR spectrum of the resulting dark green product showed evidence for heterolytic O-H activation of HCOOH because the amido donor of the ^{Ph}I$_2$P$^-$ ligand is protonated, and displayed at 5.65 ppm. In addition, the three distinct pyridine resonances, at 5.81, 5.77, and 4.92 ppm, indicate a distinct asymmetry of the dearomatized pyridine ring that we have previously observed associated with protonation of the amido.[20] Taken together, these results suggested that 1 equivalent of HCOOH had led to formation of (^{Ph}HI$_2$P$^-$)Al(OOCH)H as an initial reaction intermediate along with liberation of H_2 (Scheme 1A and Figure S7).

In addition to (^{Ph}HI$_2$P$^-$)Al(OOCH)H, the spectrum of the reaction mixture included unreacted complex **1** and a minor component that suggested the ^{Ph}I$_2$P ligand had been protonated twice. Addition of excess HCOOH:NEt$_3$ (5:2) to **1** resulted in almost complete conversion to the species containing the doubly protonated ligand. The pyridine resonances now all appear in the aromatic region 8.28 - 7.38 ppm, and we assigned the features observed at 5.23/5.33 and 5.17/5.20 ppm to C-H and N-H protons, respectively, for the two diastereomers that result from protonation of both the imino carbon and imino nitrogen atoms of ^{Ph}I$_2$P (Scheme 1A and Figure S7). Of further note, H_2 was detected by NMR and the Al-H resonance is absent in the final spectrum: this indicates that **1** has in fact reacted with three equivalents of HCOOH to afford the observed ^{1}H-NMR spectrum. The identity of the doubly protonated ligand, henceforth denoted by ^{Ph}H$_2$I$_2$P, was further confirmed using a GC-MS experiment in which a solution of the triply protonated complex was rapidly quenched with air in methanol and, following filtration through silica, GC-MS analysis indicated the presence of the aminoiminopyridine ligand (^{Ph}H$_2$I$_2$P) (Figure S8). Quenching and analysis of **1** via an identical protocol revealed only ^{Ph}I$_2$P.

Of note, analysis of a sample of the active catalyst removed during a typical experiment gave a ^{1}H-NMR spectrum and GC-MS results consistent with this same triply protonated complex which we formulate as [(^{Ph}H$_2$I$_2$P)Al(OOCH)$_2$]$^+$. Isolated complexes of H$_2$I$_2$P are rare, however the few other examples of such complexes have ^{1}H-NMR spectra that are consistent with our observations for [(^{Ph}H$_2$I$_2$P)Al(OOCH)$_2$]$^+$.[20] Similar ligand hydrogenation has also been observed in catalysts that utilize reduced α-diimine ligands to catalyse formic acid dehydrogenation and in imine catalysts for transfer hydrogenation.[21,22]

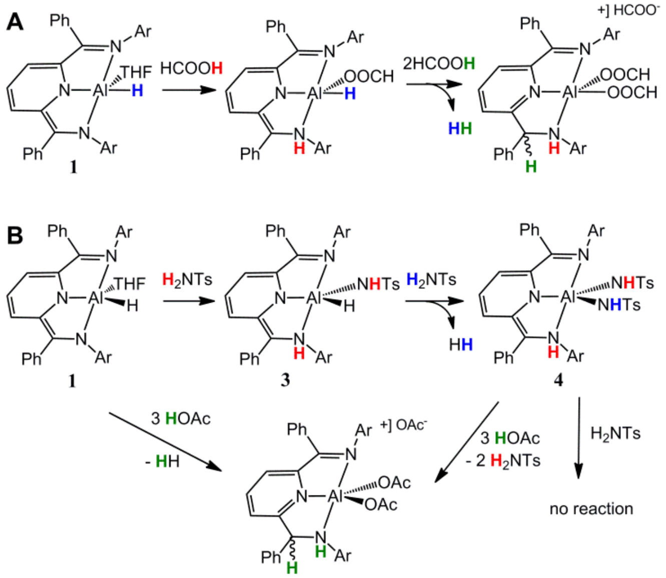

Scheme 1. (A) Products of reaction between 1 and HCOOH. (B) Reaction of 1 with weak (H$_2$NTs) and strong (HOAc) acids.

The foregoing results indicated that in the presence of HCOOH, **1** is initially protonated at the amido N atom of ^{Ph}I$_2$P, and that subsequent protonolysis of the Al-hydride and protonation of the ligand backbone at the imino C-atom occur rapidly during catalysis. However, the order of the 2nd and 3rd protonation events was indistinguishable using HCOOH as the acid (Scheme 1A). Formic acid is a strong acid and so we repeated the experiments using a weaker acid, H$_2$NTs. Addition of a single equivalent of H$_2$NTs to **1** led to the expected product (^{Ph}HI$_2$P$^-$)AlH(HNTs) (**3**) (Scheme 1B). Addition of a second equivalent of H$_2$NTs afforded protonolysis of the Al-H bond with loss of 1 equivalent of H_2, and formation of (^{Ph}HI$_2$P$^-$)Al(NHTs)$_2$ (**4**). Both **3** and **4** were characterized by ^{1}H-NMR and IR spectroscopy, and combustion analysis (Figure S9, S10). Addition of excess H$_2$NTs did not protonate the complex further; however, addition of excess acetic acid to **1** or **4** led to formation of [(^{Ph}H$_2$I$_2$P)Al(OAc)$_2$](OAc) identified by ^{1}H-NMR spectroscopy (Scheme 1B, Figure S11). These experiments indicate that catalyst **1** is first protonated at the amido N-atom, protonolysis then liberates H_2, and a 3rd equivalent of acid effects protonation at the ipso-carbon position if the acid is strong enough, such as with HCOOH or HOAc.

Characterization of β-hydride abstraction by Al(III). It is reasonable to speculate that the mechanism for liberation of CO_2 involves a β-hydride abstraction from the C-H bond in formate along with formation of an Al-hydride. To investigate the feasibility of proposing such a step in the catalytic cycle, we first studied the reverse reaction: CO_2 insertion into the Al-H bond in **1**. Insertion of CO_2 into Al-hydride bonds is reasonably rare with one previously reported example that we are aware of.[23] In the present case, exposure of **1** to 1 atm of CO_2 led to rapid formation of (^{Ph}I$_2$P^{2-})Al(κ$_2$-OOCH) (**5**) in high yield (Scheme 2). Complex **5** was characterized by single crystal X-ray diffraction, and using ^{1}H-NMR and IR spectroscopy

(Tables S2, S3, Figure 2, S12).[24] We found that **5** was stable indefinitely under heat and vacuum, and we observed no evidence for conversion back to **1** under these conditions.

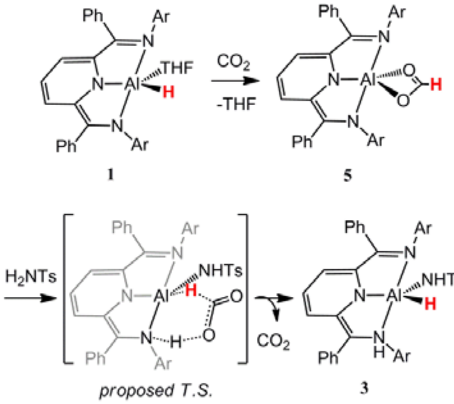

Scheme 2. Insertion and elimination of CO_2 from ($^{Ph}I_2P^{2-}$)AlH(THF) (**1**), including a proposed transition state for β-hydride abstraction that is stabilized by hydrogen bonding. The movement of the red H-atom was confirmed by deuterium labelling studies.

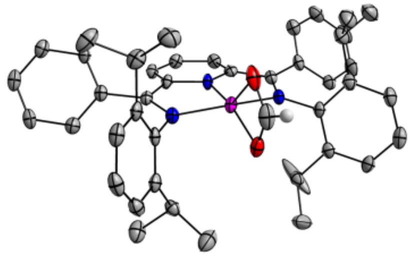

Figure 2. Structure of ($^{Ph}I_2P^{2-}$)Al(κ$_2$-OOCH) in **5**. Pink, red, blue, grey and white ellipsoids represent Al, O, N, C, and H atoms respectively. Ellipsoids are shown at the 50% probability level, hydrogen atoms except the formate hydrogen are omitted for clarity.

Addition of 1 equivalent of the weak acid H_2NTs to **5** led to rapid release of CO_2 gas and formation of ($^{Ph}HI_2P^{-}$)Al(HNTs)H (**3**) as observed by ^{1}H-NMR spectroscopy (Figure S9). Observation of **3** strongly suggested that a β-hydride abstraction reaction had occurred, and further evidence for transfer of the C-H proton from formate to form the Al-hydride was obtained using a deuterium labelled analogue of **1** (**1-D**). The deuterated analogue of **1**, ($^{Ph}I_2P^{2-}$)Al-(THF)D (**1-D**), was synthesized from $AlCl_2D$ following the same method we used to obtain **1** (*vide supra*) (Figure 3A).[24] Reaction of **1-D** with CO_2 afforded us ($^{Ph}I_2P^{2-}$)Al(κ$_2$-OOCD) (**5-D**) (Figure 3B). Exclusive formation of ($^{Ph}HI_2P^{-}$)Al(HNTs)D (**3-D**) upon reaction of **5-D** with 1 equivalent of H_2NTs confirmed that a β-hydride transfer of the formate C-H hydrogen in **5** to the Al centre in **3** had occurred (Figure 3C).

The release of CO_2 from **5** confirms that β-hydride abstraction can occur from **5** when it is singly protonated at the amido ligand of $^{Ph}I_2P^{2-}$. Our ^{1}H-NMR spectroscopy studies have shown that the active catalyst contains the doubly protonated $^{Ph}H_2I_2P$ ligand. The second protonation event occurs in the carbon backbone of the $^{Ph}H_2I_2P$ ligand and so the Al centre in this complex should have similar electronic properties to the Al complex of the singly protonated $^{Ph}HI_2P^{-}$ ligand. Consequently, we believe that β-hydride abstraction by a ($^{Ph}H_2I_2P$)Al$(OOCH)_2$ catalytic intermediate is feasible (Scheme 3).

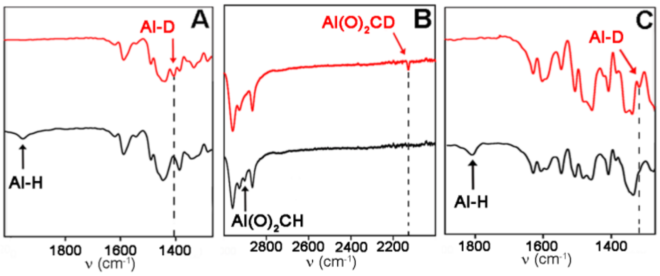

Figure 3. (**A**) IR spectra of **1** (black), and **1-D** (red). (**B**) IR spectra of **5** (black), and **5-D** (red). (**C**) IR spectra of **3** (black), and **3-D** (red). Stretching frequencies for the Al-D and C-D stretches matched predicted values, which are marked with dashed lines (Calculation S1).

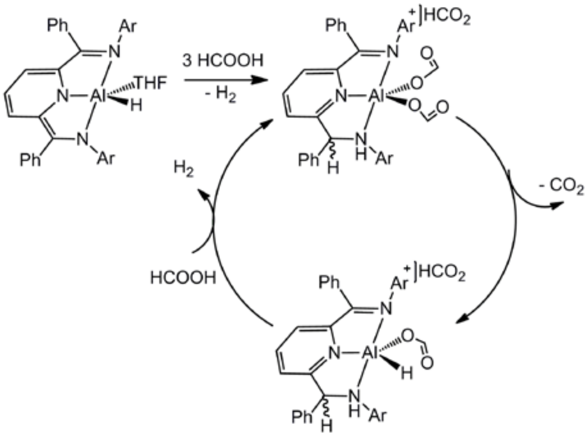

Scheme 3. Proposed mechanism for HCOOH dehydrogenation by **1**.

Based on analogies to previously reported work involving β-hydride abstraction by acidic transition metal ions, the transition state for β-hydride abstraction during catalysis by **1** most likely resembles "outer sphere β-hydride abstraction".[25,26] In these situations, a hydrogen-bonded 6-membered ring defines the transition state for hydride transfer (Scheme 2). There are two major factors that suggest to us that the observed β-hydride abstraction follows this pathway: 1) β-hydride abstraction from the aluminium-bound formate ligand requires that the $^{Ph}I_2P^{2-}$ ligand be protonate: insertion of CO_2 is favoured when $^{Ph}I_2P^{2-}$ is unprotonated as in **1**, while β-hydride transfer to afford the Al-hydride is favoured when $^{Ph}I_2P^{2-}$ is singly or doubly protonated, as in the reaction of **5** with H_2NTs, or during formic acid dehydrogenation catalysis, respectively. It is likely that protonation of the amido donor of $^{Ph}I_2P^{2-}$ provides stabilization of the β-hydride abstraction transition state via hydrogen bonding (Scheme 2). As a specific example, molecular Ir complexes of hydroxide-substituted bipyridine ligands also favour insertion and CO_2 hydrogenation in their deprotonated state, and HCOOH dehydrogenation in their protonated form;[13] 2) Early metal acidic catalysts that undergo traditional β-hydride elimination are inhibited by donor solvents due to competitive binding to open coordination sites, while "outer sphere β-hydride abstraction" is accelerated in donor solvents that stabilize the hydrogen-bonded transition states.[15,16,27,28] The dehydrogenation catalysis that we observed in donor solvents such as THF (*vide supra*) lends further support to the proposal that "outer sphere β-hydride abstraction" is operative for the β-hydride abstraction step in the dehydrogenation of HCOOH by **1** and **2**.

Summary of Proposed Mechanism for HCOOH Dehydrogenation. Considering all of the experimental evidence that we have described, we propose that under the catalytic conditions for dehydrogenation of HCOOH, **1** exists with the $^{Ph}I_2P^{2-}$ ligand in a doubly protonated form: $[(^{Ph}H_2I_2P)Al(OOCH)_2]^+$. β-hydride abstraction from this resting state affords an Al-hydride intermediate, $[(^{Ph}H_2I_2P)Al(OOCH)H]^+$ which quickly releases H_2 upon protonation by more HCOOH (Scheme 3).

The mechanism for deactivation of **1** during catalysis was probed using GC-MS and IR spectroscopy. In each case the decomposition products were identified as $^{Ph}H_2I_2P$ by GC-MS and $Al(HCOO)_3$ by IR spectroscopy. These decomposition products suggested that the deactivation pathway for the catalyst is the displacement of the neutral H_2I_2P ligand from the aluminium centre which leads to formation of insoluble $Al(HCOO)_3$. Based on this insight, synthesis of aluminium complexes with new ligands to stabilize aluminium(III) complexes more effectively is underway.

Conclusions and Outlook.

We have demonstrated that a molecular aluminium complex selectively catalyses the dehydrogenation of formic acid into H_2 and CO_2, with an initial turnover frequency of 5200 turnover/h. This reactivity is enabled by the ability of **1** to perform facile β-hydride abstraction from the formate anion to generate an Al-hydride intermediate and liberate CO_2. Stoichiometric reactions between **1** and CO_2 have established that insertion of CO_2 into an Al-hydride bond of **1** is favoured in the absence of a proton source, while β-hydride abstraction of formate is favoured upon protonation of the catalyst. Together these observations are consistent with a hydrogen bond-stabilized transition state that gives access to unusually facile β-hydride abstraction for an aluminium complex. The knowledge we have gained regarding facile β-hydride abstraction at Al will be applied to other chemical transformations.

Experimental Section.

Physical Measurements. Elemental analyses were performed by Columbia Analytical. ^{1}H-NMR spectra were recorded at ambient temperature (unless otherwise noted) using a Varian 600 MHz spectrometer. Chemical shifts were referenced to residual solvent. IR spectra were recorded with a Bruker-ALPHA FT-IR spectrometer with a universal sampling module and KBr pellet. GC-MS measurements were conducted on an Agilent 6890N GC with a 5973N MSD and a Varian FactorFour Capillary Column (VF-5ms, 30M x 0.25MM ID DF=0.25). Gas measurements were conducted on a Varian 3800 GC with a thermal conductivity detector (TCD).

X-ray Structure determinations. X-ray diffraction studies were carried out on a Bruker SMART APEX Duo diffractometer equipped with a CCD detector.[29] Measurements were carried out at -175 °C using Cu K_α (1.54178 Å) radiation. Crystals were mounted on a glass capillary or Kaptan Loop with Paratone-N oil. Initial lattice parameters were obtained from a least-squares analysis of more than 100 centred reflections; these parameters were later refined against all data. Data were integrated and corrected for Lorentz polarization effects using SAINT[29] and were corrected for absorption effects using SADABS2.3.[29]

Space group assignments were based upon systematic absences, E statistics, and successful refinement of the structures. Structures were solved by direct methods with the aid of successive difference Fourier maps and were refined against all data using the SHELXTL 5.0 software package.[29] Thermal parameters for all non-hydrogen atoms were refined anisotropically. Hydrogen atoms, where added, were assigned to ideal positions, and refined using a riding model with an isotropic thermal parameter 1.2 times that of the attached carbon atom (1.5 times for methyl hydrogens).

Preparation of Compounds. All manipulations were carried out using standard Schlenk or glove-box techniques under a dinitrogen atmosphere. Unless otherwise noted, solvents were deoxygenated and dried by thorough sparging with Ar gas followed by passage through an activated alumina column. Deuterated solvents were purchased from Cambridge Isotopes Laboratories, Inc. and were degassed and stored over activated 3 Å molecular sieves prior to use. $^{Ph}I_2P$ and **1** were synthesized according to literature methods.[24,30] Anhydrous formic acid was purified by drying over boric anhydride followed by fractional distillation.[31] $LiAlD_4$ was purchased from sigma Aldrich and used without further purification. All other reagents were purchased from commercial vendors and used without further purification.

$(^{Ph}I_2P^{2-})Al(CH_3)(THF)$ (2). Sodium metal (50.0 mg, 2.10 mmol) was added to a solution of $^{Ph}I_2P$ (606 mg, 1.00 mmol) in THF (15 mL) and the resulting solution was stirred for 24 hours during which time it changed first to a dark green colour and ultimately to a deep purple colour. To the dark purple solution, $AlCl_2(CH_3)$ (1M in hexane, 1.0 mL, 1.00 mmol) was added carefully. The resulting brown solution was stirred for 1 hour, the solvent was removed in vacuo, and the resulting solid was extracted into benzene (20 mL) and filtered through celite. The solution was evaporated to dryness, dissolved in minimal THF and hexane (5 mL) was layered on top and the resulting solution was cooled at -25 °C overnight to collect $(^{Ph}I_2P^{2-})Al(CH_3)(THF)$ 2 (499 mg, 68%). Complex **2** was identified by its ^{1}H-NMR spectrum. ^{1}H-NMR (600 MHz, C_6D_6): 6.89-7.12 (m, 16H, ph), 6.48 (d, *J* = 7.1, 2H, py), 5.67 (t, *J* = 6.8, 1H, py), 3.49 (br, 4H, THF), 3.17 (sept, *J* = 7.5, 4H, $CH(CH_3)_2$), 1.32 (br, 4H, THF), 1.26 (d, *J* = 7.5, 12H, $CH(CH_3)_2$), 1.04 (d, *J* = 7.5, 12H, $CH(CH_3)_2$), -0.51 (s, 3H, Al-CH_3) δ IR (KBr): 1595 (s, im) cm^{-1}. Anal. Calcd. for $C_{48}H_{57}AlN_3O$: C, 80.19; H, 7.99; N, 5.84. Found: C, 79.92; H, 7.84; N, 5.51.

(^{Ph}HI$_2$P$^-$)AlH(HNTs) (3). H$_2$NTs (171 mg, 1.00 mmol) was added to a solution of **1** (630 mg, 1.00 mmol) in toluene (10 mL), and stirred for 1 hour until the solution was a uniform purple colour. The solvent was removed *in vacuo* and the resulting solid was washed with cold hexane (2 mL) to remove trace organics. The resulting solid was extracted into hexane and cooled overnight at -25°C to precipitate (^{Ph}HI$_2$P$^-$)AlH(NTs) (**3**) (489 mg, 61%) as a purple powder. ^{1}H-NMR (600 MHz, C$_6$D$_6$): 6.47 (d, *J* = 7.0, 1H, py), 5.84 (dd, *J* = 7.0, 4.1, 1H, py), 5.67 (s, 1H, NH), 5.38 (d, *J* = 7.0, 1H, py), 4.48 (s, 1H, N*H*Ts), 4.36 (br, 1H, Al-H), 4.06 (sept, *J* = 8.2, 1H, *CH*(CH$_3$)$_2$), 3.59 (sept, *J* = 8.3, 1H, *CH*(CH$_3$)$_2$), 3.36 (sept, *J* = 8.1, 1H, *CH*(CH$_3$)$_2$), 2.83 (sept, *J* = 8.1, 1H, *CH*(CH$_3$)$_2$), 2.14 (s, 3H, NHTs), 1.94 (d, 6H, CH(CH_3)$_2$), 1.86 (d, 6H, CH(CH_3)$_2$), 1.77 (d, 6H, CH(CH_3)$_2$), 1.64 (d, 6H, CH(CH_3)$_2$), 1.59 (d, 6H, CH(CH_3)$_2$), 1.49 (d, 6H, CH(CH_3)$_2$), 1.37 (d, 6H, CH(CH_3)$_2$), 0.73 (d, 6H, CH(CH_3)$_2$) δ. IR (KBr): 3364 (m, NH, NHTs), 3265 (m, NH, ^{Ph}HI$_2$P$^-$), 1807 (w, Al-H), 1621 (m, im), 1598 (m, im), 1589 (m, im), 1386 (m, S=O), 1162 (m, S=O) cm^{-1}. Anal. Calcd. for $C_{50}H_{57}AlN_4O_2S$: C, 74.60; H, 7.14; N, 6.96. Found: C, 74.12; H, 6.75; N, 7.22.

(^{Ph}HI$_2$P$^-$)Al(HNTs)$_2$ (4). H$_2$NTs (342 mg, 2.00 mmol) was added to a solution of **1** (630 mg, 1.00 mmol) in toluene (10 mL). The resulting solution was stirred for 24 hours until the solution was a uniform purple colour. The solvent was removed *in vacuo* and the resulting solid was washed with cold hexane (2 mL) to remove trace organics. The resulting solid was extracted into hexane and cooled overnight at -25°C to precipitate (^{Ph}HI$_2$P$^-$)Al(HNTs)$_2$ (**4**) (506 mg, 51%) as a purple powder. ^{1}HNMR (600 MHz, C$_6$D$_6$): 6.49 (d, *J* = 7.0, 1H, py), 5.82 (dd, *J* = 7.0, 4.3, 1H, py), 5.59 (s, 1H, NH), 5.37 (d, *J* = 7.0, 1H, py), 4.61 (s, 1H, N*H*Ts), 4.53 (s, 1H, N*H*Ts), 3.84 (sept, *J* = 8.1, 1H, *CH*(CH$_3$)$_2$), 3.31 (sept, *J* = 8.1, 1H, *CH*(CH$_3$)$_2$), 3.09 (sept, *J* = 8.1, 1H, *CH*(CH$_3$)$_2$), 2.57 (sept, *J* = 8.1, 1H, *CH*(CH$_3$)$_2$), 2.14 (s, 3H, NHTs), 2.01 (s, 3H, NHTs), 0.93-1.51 (m, 24H, CH(CH_3)$_2$) δ. IR (KBr): 3389 (w, NH, NHTs), 3375 (m, NH, NHTs), 3260 (m, NH, ^{Ph}HI$_2$P$^-$), 1621 (m, im), 1598 (m, im), 1589 (m, im), 1386 (m, S=O), 1162 (m, S=O) cm^{-1}. Anal. Calcd. for $C_{50}H_{57}AlN_4O_2S$: C, 70.27; H, 6.62; N, 7.19. Found: C, 70.11; H, 6.87; N, 7.01.

(^{Ph}I$_2$P^{2-})Al(κ^2-OOCH) (5). Dry CO$_2$ was sparged through a solution of **1** (630 mg, 1.00 mmol) in benzene (5 ml). The reaction was stirred for 1 hour before the solvent was removed in vacuo. The resulting red-brown solid was extracted into hexane (20 mL) and filtered through Celite. The solution was concentrated to 10 mL and chilled overnight at -25° C. Red-brown (^{Ph}I$_2$P^{2-})Al(κ^2-OOCH) (**5**) (571 mg, 84%) was collected as single crystals suitable for X-ray diffraction. ^{1}H-NMR (600 MHz, C$_6$D$_6$): 6.91-7.13 (m, 16H, ph), 6.83 (d, *J* = 6.8, 2H, py), 6.61 (s, 1H, OOCH), 5.66 (t, *J* = 6.9, 1H, py), 3.12 (sept, *J* = 7.8, 4H, *CH*(CH$_3$)$_2$), 1.29 (d, *J* = 7.7, 12 H, CH(CH_3)$_2$), 0.81 (d, *J* = 7.7, 12H, CH(CH_3)$_2$)) δ. IR (KBr): 2901 (w, OOCH) 1656 (m, OOCH), 1622 (m, im), 1585 (s, im) cm^{-1}. Anal. Calcd. for $C_{44}H_{48}AlN_3O_2$: C, 77.96; H, 7.14; N, 6.20. Found: C, 77.82; H, 7.05; N, 6.33.

(^{Ph}I$_2$P^{2-})AlD(THF) (1-D). Compound **1-D** was synthesized in an analogous manner to **1** using a mixture of LiAlD$_4$ and AlCl$_3$ in place of LiAlH$_4$ and AlCl$_3$.[20] The ^{1}H-NMR spectrum was consistent with the spectrum of **1** with the exception of the Al-H resonance which was diminished in intensity. IR (KBr): 1418 (w, Al-D) cm^{-1}.

(^{Ph}HI$_2$P$^-$)AlD(HNTs) (3-D). Pure compound **3-D** was synthesized in an analogous manner to **3** using **1-D** in place of **1**. The ^{1}H-NMR spectrum was consistent with the spectrum of **3** with the exception of the Al-H resonance which was diminished in intensity. IR (KBr): 1307 (w, Al-D) cm^{-1}.

(^{Ph}I$_2$P^{2-})Al(κ^2-OOCH) (5-D). Compound **5-D** was synthesis in an analogous manner to **5** using **1-D** in place of **1**. The ^{1}H-NMR spectrum was consistent with the spectrum of **5** with the exception was the formate C-H resonance which was greatly diminished in intensity. IR (KBr): 2129 (w, OOCD) cm^{-1}.

Reaction of 5-D with H$_2$NTs. **5-D** (60.3 mg, 0.1 mmol) in toluene (2 mL) was reacted with H$_2$NTs (17.1 mg, 0.1 mmol). The reaction was stirred for 1 hour until the solution was a uniform purple colour. Analysis of the headspace gasses by GC-TCD revealed the release of CO$_2$ gas. The resulting solution was evaporated to dryness and identified as **3-D** by ^{1}H-NMR and IR spectroscopy.

Typical procedure for the dehydrogenation of HCOOH. Compound **1** (7.1 mg, 0.010 mmol) was dissolved in dry, degassed THF (5 mL) in a 250 mL 3 neck flask equipped with an addition funnel. The apparatus was transferred to the Schlenk line and outfitted to allow for gas collection (Figure S13). The solution was heated to 65°C. It was essential that the catalyst remain dark brown in colour after reaching thermal equilibrium. Contamination by protic species led to blue green solutions, while oxidation led to yellow solutions. Degassed 5:2 HCOOH:NEt$_3$ (2 mL) was transferred to the addition funnel and added under a flow of nitrogen to the solution. After complete addition of the formic acid the flow of nitrogen was ceased and the volume of gas produced was monitored. Conversion of volume of gas produced to moles of gas produced was accomplished using the Van de Waals equation along with corrections for the vapour pressure of water as well as the difference in liquid height in the burette and surrounding reservoir.

Acknowledgements

We thank the University of California Davis for support of this work. L.A.B. is an Alfred P. Sloan Foundation Fellow.

Notes and references

[a] Department of Chemistry, University of California Davis, California 95615, United States

Electronic Supplementary Information (ESI) available: 1HNMR spectra, GC-TCD analysis, GCMS analysis, kinetic data, reduced mass calculations, CCDC 994956. For ESI and crystallographic data in CIF and other electronic format see DOI: 10.1039/b000000x/

---

[1] Group 13 Chemistry III Industrial Applications (H. W. Roesky, D. A. Atwood Eds.), Springer (2003) Berlin.

[2] P. H. M. Budzelaar, G. Talarico, *Insertion and β-Hydride Transfer at Aluminium*, in Group 13 Chemistry III Industrial Applications (H. W. Roesky, D. A. Atwood Eds.), Springer (2003) Berlin. p141 -167.

[3] a) R. B. Woodward, N. L. Wendler, F. J. Brutschy, *J. Am. Chem. Soc.* 1945, **67**, 1425. b) A. G. Guimanini, A. Drusiani, L. Plessi, *J. Org. Chem.* 1975, **12**, 1845. c) G. Talarico, P. H. M. Budzelaar, A. W. Gal, *J. Comp. Chem.* 2000, **5**, 398.

[4] T. Mole, E. A. Jeffery *Organoaluminium Complexes***,** 1972, Elsevier, Amsterdam.

[5] W. M. Haynes, Ed. *CRC Handbook of Chemistry and Physics*, 91st ed. CRC: Boca Raton, 2010; p 4-1.

[6] P. P. Power, *Nature*, 2010, 463, 171.

[7] M. M. Hansmann, R. L. Melen, D. S. Wright, *Chem. Sci.* 2011, **2**, 1554.

[8] C. Appelt, J. C. Slootweg, K. Lammertsma, W. Uhl, *Angew. Chem. Int. Ed.* 2013, **52**, 4256.

[9] a) W. Uhl, *Anorg. Allorg.* 1989, **570**, 37. b) W. Uhl, A. Vester, Chem. Ber. 1993, 126, 941. c) W. Uhl, L. Marcus, *Z. Anorg. Allorg.* 1994, **620**, 1427.

[10] a) J. A. Turner, *Science*, 2004, **305**, 972. b) L. Schlapbach, A. Züttel, *Nature*, 2001, **414**, 353. c) T. C. Johnson, D. J. Morris, M. Wills, *Chem. Soc. Rev.* 2010, **39**, 81.

[11] a) M. Grasemann, G. Laurenczy, *Energy. Environ. Sci.*, 2012, **5**, 8171. b) E.Fujita, J.T. Muckerman, Y. Himeda, *Biophysica Acta*, 2013, **1827**, 1031. c) R. Tanaka, M. Yamashita, K. Nozaki, *J. Am. Chem. Soc.*2009, **131**, 14168. d) Y. Himeda, *Green Chem.* 2009, **11**, 2018. e) S. Fukuzumi, T. Kobayashi, T. Suenobu, *J. Am. Chem. Soc.* 2010, **132**, 11866. f) R. Tanaka, M. Yamashita, L. W. Chung, K. Morokuma, K. Nozaki, *Organometallics*, 2011, **30**, 6743. g) J. F. Hull, Y. Himeda, W. H. Wang, B. Hashiguchi, R. Periana, D. J. Szalda, J. T. Muckermann, E. Fujita, *Nature Chem.* 2012, **4**, 383. h) J. H. Barnard, C. Wang, N. G. Berry, J. Xiao, *Chem. Sci.* 2013, **4**, 1234. i) Y. Manaka, W. H. Wang, Y. Suna, H. Kambayashi, J. T. Muckerman, E. Fujita, Y. Himeda, *Catal. Sci. Technol.* 2014, **4**, 34. j) S. Oldenhof, B. de Bruin, M. Lutz, M. A. Siegler, F. W. Patureau, J. I. V. D. Vlugt, J. N. H. Reek, *Chem. Eur. J.* 2013, **19**, 11507.

[12] a) C. Fellay, P. J. Dyson, G. Laurenczy, *Angew. Chem. Int. Ed.* 2008, **47**, 3966. b) T. Koike, T. Ikariya, *Adv. Synth. Catal.* 2004, **346**, 37. c) Y. Gao, J. K. Kuncheria, H. A. Jenkins, R. J. Puddephatt, G. P. A. Yap, *Dalton Trans.* 2000, 3212. d) W. Gan, C. Fellay, P. J. Dyson, G. Laurenczy, *J. Coord. Chem.* 2010, **63**, 2685.

[13] D. J. Morris, G. J. Clarkson, M. Wills, *Organometallics*, 2009, **28**, 4133.

[14] M. Vogt, A. Nerush, Y. Diskin-Posner, Y. Ben-David, D. Milstein, *Chem. Sci.* **2014**, advance article.

[15] Kudrik, E. V.; Makarov, S. V.; Ageeva, E. S.; Dereven'kov, I. A. *Macroheterocycles*, 2009, **2**, 69.

16 a) Boddien, A.; Mellmann, D.; Gärtner, F.; Jackstell, R.; Junge, H.; Dyson, P. J.; Laurenczy, G.; Ludwig, R.; Beller, M. *Science*, 2011, **333**, 1733. b) Zell, T.; Butscheke, B.; Ben-David, Y.; Milstein, D. *Chem. Eur. J.* 2013, *19*, 8068.

[17] T. W. Myers, Berben, L. A. *J. Am. Chem. Soc.* 2013, **135**, 9988.

[18] G. Lente, Response to A. Boddien, D. Mellmann, F. Gärtner, R. Jackstell, H. Junge, P. J. Dyson, G. Laurenczy, R. Ludwig, M. Beller, *Science*, 2011, **333**, 1733.

[19] S. Kozuch, J. M. I. Martin, *ACS Catal.*, 2012, **2**, 2787.

[20] N. Cosquer, B. Le Gall, F. Conan, J.-M. Kerbaol, J. Sala-Pala, M. M. Kubicki, E. Vigier, *Inorg. Chim. Acta.* 2006, **359**, 4311.

[21] R. E. Rodríguez-Lugo, M. Trincado, M. Vogt, F. Tewes, G. Santiso-Quinones, H. Grützmacher, *Nature Chem.* 2013, **5**, 342.

[22] W. Zuo, A. J. Lough, Y. F. Li, R. H. Morris, *Science*, 2013, **342**, 1080.

[23] P.C. Kuo, I.-C. Chen, J.-C. Chang, C.-H. Hu, C.-H. Hung, H. M. Laee, J.-H. Huang, *Eur. J. Inorg. Chem.* 2004, 4898.

[24] W. Sattler, G. Parkin, *J. Am. Chem. Soc.* 2011, **133**, 9708.

[25] S. E. Clapham, A. Hadzovic, R. H. Morris, *Coord. Chem. Rev.*, 2004, **248**, 2201.

[26] R. Noyori, M. Yamakawa, S. Hashiguchi, *J. Org. Chem.*, 2001, **66**, 7931.

[27] P. J. Chirik, J. E. Bercaw, *Organometallics*, 2005, **24**, 5407.

[28] J. Spielmann, G. Jansen, H. Bandmann, S. Harder, *Angew. Chem. Int. Ed.* 2008, **47**, 6290.

[29] a) SMART Software Users Guide, Version 5.1, Bruker Analytical X-ray Systems, Inc. (1999) Madison, WI. b) SAINT Software Users Guide, Version 7.0, Bruker Analytical X-Ray Systems, Inc. (1999) Madison, WI. c) Sheldrick, G. M. SADABS, Version 2.03, Bruker Analytical X-Ray Systems, Inc. (2000) Madison, WI. d) Sheldrick, G. M. SHELXTL Version 6.12, Bruker Analytical X-Ray Systems, Inc. (1999) Madison, WI.

[30] N. Kleigrewe, W. Steffen, T. Blömker, G. Kehr, R. Fröhlich, B. Wibbeling, G. Erker, J-C. Wasilke, G. Wu, G. C. Bazan, *J. Am. Chem. Soc.*, 2005, **127**, 13955.

[31] J. H. Walton, C. K. Rosenbaum, *J. Am. Chem. Soc.* 1928, **50**, 1648.

Selective conversion of formic acid to H_2 and CO_2 is catalysed by a molecular aluminum complex. Metal-ligand cooperative interactions stabilize a transition state for an outer-sphere β-hydride abstraction mechanism for catalysis.